J. Phys. Earth, **39**, 345–360, 1991

Seismic Ray Focusing around the Magma Reservoir beneath the Eastern Part of Izu Peninsula, Honshu, Japan

Tameshige Tsukuda

Earthquake Research Institute, The University of Tokyo,
Bunkyo-ku, Tokyo 113, Japan

Azimuthal variation of P amplitudes from a volcanic earthquake observed at distant stations is interpreted in terms of focusing and defocusing of seismic rays propagating through the low-velocity body around the magma reservoir beneath the region of high crustal activity near the east coast of Izu Peninsula, central Honshu, Japan. Numerical ray tracing was carried out for the models of spherical and cylindrical low-velocity bodies. The P velocity within the body is assumed to be lowered by a certain amount compared with the surrounding medium. The center of the reservoir was inferred to be located at around the northeastern end of the area of the Higashi-Izu monogenetic volcanoes and at a depth of 10 to 20 km. The radius of the low-velocity body is 10 km containing a 3 km radius core of 3–4% lower velocity.

1. Introduction

The east coast region of Izu Peninsula, central Honshu, has been frequently attacked by severe earthquake swarms in recent years since 1978 (e.g., JMA, 1990). The source areas are distributed from just around Ito City to several tens of kilometers off the city. On July 13, 1989, this activity was accompanied by a submarine volcanic eruption at Teisi Knoll. Thus the anomalous seismicity turned out to be closely related to the volcanic activity. A similar remarkable swarm activity took place in the same area in 1930 (Nasu, 1935). Kuno (1954) previously proposed an idea that such an earthquake swarm as the 1930 event was caused by the subsurface magmatic activity which is evidenced by the presence of Omuro-yama volcano group. The ground uplift centering around the eastern Izu Peninsula in recent years measured by Geographical Survey Institute of Japan (e.g., GSI, 1978; Ishii, 1989) is also considered to be due to the expansion of the subsurface magma reservoir (Hagiwara, 1977).

To make clear the position and the size of the deep magmatic region, it may be quite effective to study the seismic waves propagating through it. Fortunately, a seismic event most suitable for the purpose happened on November 16, 1987, the eruption of Izu-Oshima Volcano. Impulsive P waveforms with an anomalous amplitude distribution were observed at the distant stations with nearly the same epicentral distances for a certain azimuthal range (Figs. 1 and 2). In this paper, we shall show that focusing and

Received October 31, 1990; Accepted January 21, 1991

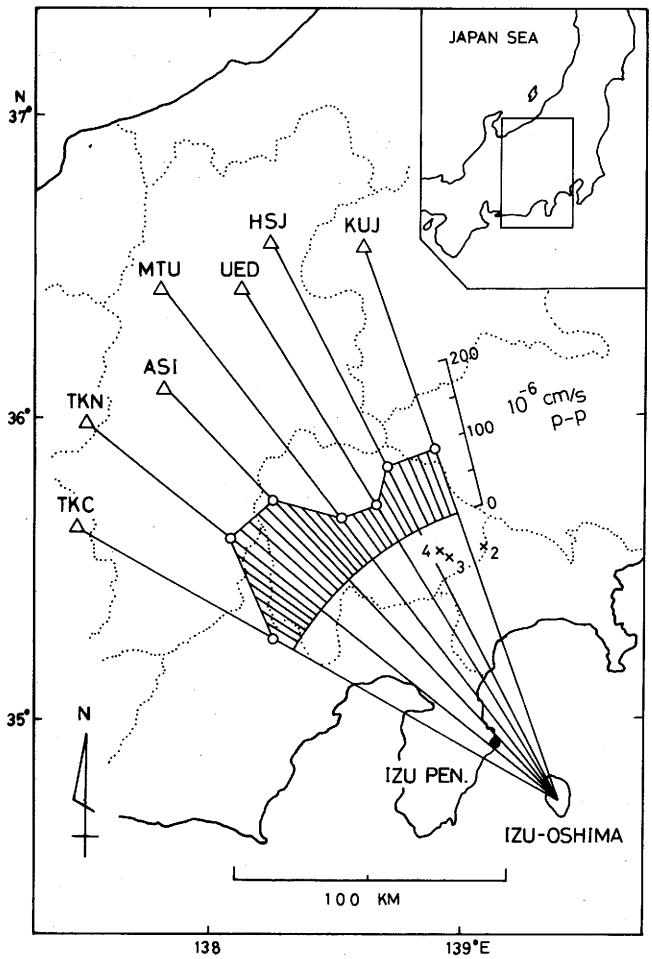

Fig. 1. Map showing the region concerned and locations of seismic stations together with the normalized azimuthal amplitude distribution of P waves from the eruption of the Izu-Oshima Volcano on November 16, 1987, at 10:47 (JST). Dotted line is the prefectural border. Solid circle at the east coast of Izu Peninsula indicates the proposed position of the magma reservoir. The observed peak-to-peak amplitudes are multiplied by $r/200$, where r is epicentral distance in km. The epicenters listed in Table 1 are shown by × with their event numbers.

defocusing of seismic rays propagating through a low-velocity body explains the amplitude variation fairly well.

2. Observation: Anomalous Amplitudes and Travel Times

The sequence of eruptions of Volcano Mihara in Izu-Oshima Island from November 1986 to November 1987 emitted numerous characteristic seismic waves. In particular, the eruption on November 16, 1987, at 10:47 (JST), generated the most prominent P waves that were recorded on the velocity-type seismographs (Fig. 2). The initial motions show all compression indicative of an explosive or single force focal mechanism. The observation stations are located at epicentral distances of about 200 km in the direction between N59.0°W and N18.4° W from the epicenter. Despite this relatively narrow azimuthal range the normalized peak-to-peak amplitudes for the first cycle of the initial wavelet show strong azimuthal variation: The maximum difference amounts to about a factor of 3 (Fig. 1).

The spectra of these P wavelets shown in Fig. 3 have a peak at 0.6–0.7 Hz, while the other volcanic seismic events have oscillatory waves with predominant frequencies higher than 1.3 Hz. The waveform from HSJ contains high frequency components

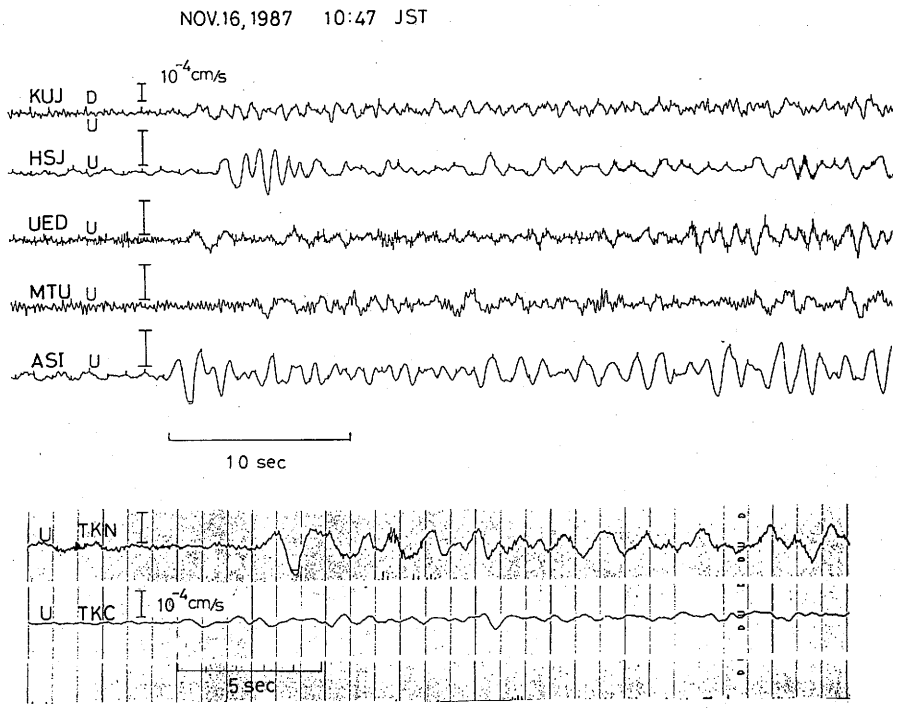

Fig. 2. Vertical component waveforms from the eruption recorded at the stations shown in Fig. 1. The amplitude frequency characteristic is nearly flat from 1 to 30 Hz in particle velocity on the ground. The upper five seismograms are from the Shin'etsu Seismological Observatory, Earthquake Research Institute, the University of Tokyo, whereas the lower two are from the Observation Center for Earthquake Prediction, Faculty of Science, Nagoya University.

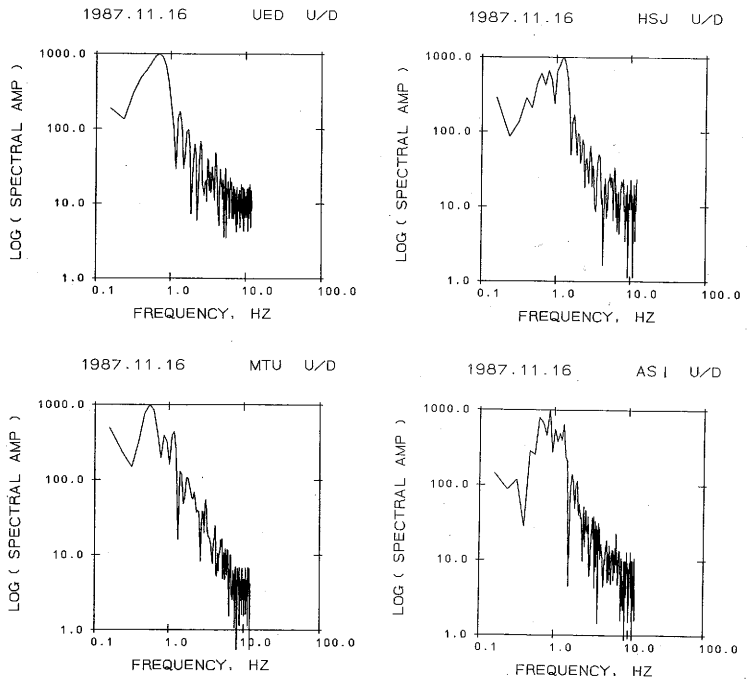

Fig. 3. Amplitude spectra for the eruption seismic waves. P wave group during 8 s from the onset is processed by FFT (Fast Fourier Transform).

immediately after the low frequency first wave as found in Figs. 2 and 3. We shall concentrate on these low frequency waves, which have an advantage that they are only slightly affected by the small-scale irregular structures like soft layers near the ground surface.

We ought to locate the hypocenter of the event from the viewpoint of volcanology. For the seismic waves recorded in the island, which are from the network set up by the Izu-Oshima Volcano Observatory, the University of Tokyo, are all clipped in the part of its occurrence and we cannot read the arrival times. The eruption that excited these prominent seismic waves has been studied analyzing the crustal deformation and the seismicity around the summit crater of the volcano and is considered to be the result of magma drain-back (Ida *et al.*, 1988 b; Yamaoka *et al.*, 1989; Takeo *et al.*, 1990). The epicenter is probably at the summit crater of Mt. Mihara. Since gravity survey suggested that the collapsed portion of the magma chamber due to the lava drain-back is to be around the sea level (Watanabe *et al.*, 1988), the depth of the hypocenter of this event would be shallower than several kilometers (Fukuyama and Takeo, 1990). We assume it as 1km here. The origin time was estimated by comparing between observational and theoretical travel times at distant stations as described below. The hypocentral parameters are listed in Table 1. The teleseismic event occurred 14.0 s earlier than the eruption time estimated by Yamaoka *et al.* (1989) through the arrival times of the volcanic air shocks.

Table 1. Hypocentral parameters of the eruption earthquake (No. 1) at Mt. Mihara in Izu-Oshima Island and earthquakes (Nos. 2 to 4) originating in the eastern part of Yamanashi Prefecture used for estimating station correction terms for travel times. The origin time in parenthesis for No.1 event is the eruption time.

No.	Origin time (JST)	Longitude (°E)	Latitude (°N)	Depth (km)	Magnitude
1	Nov. 16, 1987, 10:47:12.7 (10:47:26.7)	139.398	34.723	1.0	
2	Oct. 18, 1987, 03:41:10.82	139.1054	35.5634	17.4	4.7
3	Sept. 5, 1988, 00:49:22.37	138.9468	35.5365	22.0	5.4
4	Sept. 5, 1988, 07:31:01.30	138.9243	35.5518	18.3	4.3

As mentioned above, the seismograms from the University of Tokyo are not complete. Therefore, the radiation pattern of the prominent P waves at the source cannot be strictly confirmed by the seismic records at the stations of short distances and of various directions. Only available near-field seismograms are obtained at a station attached to the National Research Institute for Earth Science and Disaster Prevention, 1.8 km northwest from the crater, equipped with a three-component digital seismograph with wide-amplitude and wide-frequency range (Fukuyama and Takeo, 1990). The waves have predominant radial components. Meanwhile, Japan Meteorological Agency had installed volumetric strain meters in the Tokai and southern Kanto areas, which provided long-period seismograms for the concerned event. The maximum amplitudes, which are from Rayleigh waves with a predominant period of several tens of seconds, are almost constant for a wide range of azimuth (Takeo *et al.*, 1990). The facts of uniform radiation of Rayleigh waves and weak excitation of transverse component near-field seismic waves support an azimuthally isotropic radiation pattern, although the frequency ranges are different from that of our waveforms. Fukuyama and Takeo (1990) and Takeo *et al.* (1990) presented a vertical single force source model utilizing the near-field and far-field waveform data, respectively.

In addition to the amplitude anomalies, significant travel time anomalies were observed. They involve contributions from the various parts of the medium. To see the effect of the local velocity structure just beneath the stations, we need earthquake events having similar ray paths toward the stations with the Mt. Mihara event. The shocks that originated at the eastern Yamanashi Prefecture with their focal depths of around 20 km are quite appropriate for this purpose (Table 1). The P velocity structure model used for determining hypocenters and calculating theoretical travel times is given in Fig. 4(a). This 1-D model is constructed in reference to the 3-D heterogeneous structure derived by Ashiya *et al.* (1987). The velocity gradient is to be constant within the layers. Calculated O-C residuals are namely the travel time anomalies arising from the medium toward the stations, which are regarded as station correction terms for the travel time study for the medium beneath the Izu-Oshima region. Subtracting these residuals from the arrival times for the eruption event, we obtain the anomalies for the half path from the source. Table 2 shows the results. Here, the origin times of the seismic event were calculated assuming that the average O-C times should be zero.

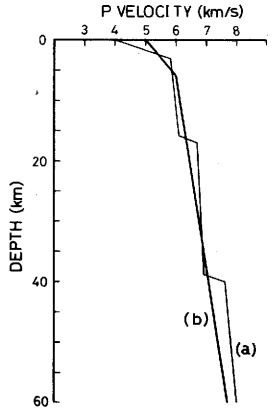

Fig. 4. Standard P velocity structure models used for (a) the travel time study and (b) the ray tracing. The velocity varies linearly within layers.

Table 2. Travel time anomalies for the volcanic earthquake (No. 1 in Table 1). The azimuth is taken from the north clockwise. The reading errors for the onset of this event are $\pm 0.1 - \pm 0.2$ s.

Station	Distance (km)	Azimuth (°)	Station correction (s)	Travel time residual (s)
KUJ	216.4	−18.4	0.23 ± 0.30	
HSJ	230.2	−25.9	0.28 ± 0.28	−0.08
UED	219.6	−30.6	0.31 ± 0.17	−0.27
MTU	237.1	−36.1	0.68 ± 0.13	−0.05
ASI	209.3	−41.7	0.33 ± 0.25	0.09
TKN	219.4	−49.9	0.14 ± 0.28	0.56
TKC	203.7	−59.0	0.12	0.38

3. Numerical Simulation: Ray Tracing on a Low-Velocity Body

As the high amplitudes emerged behind the magmatic region around the eastern part of Izu-Peninsula, we are struck with an idea of focusing of seismic rays bent during their propagation due to velocity gradient (e.g., Jackson, 1971). The focusing center is located somewhere between the two lines: from the Izu-Oshima Volcano to the stations TKN and ASI. We shall try to make a numerical simulation on a low-velocity body model to explain the anomalous amplitude distribution.

We ought to set up some assumptions concerning the seismic source: the hypocenter is given in Table 1; the radiation strength is nearly the same for an observational range of azimuth provided the range of take-off angles at the source is small enough. Furthermore, we assume the velocity structure: a simple model as given in Fig. 4(b) is adopted for the standard medium model in order to avoid complexity on the interfaces where conversion and reflection of seismic waves occur. Two kinds of shape are modeled

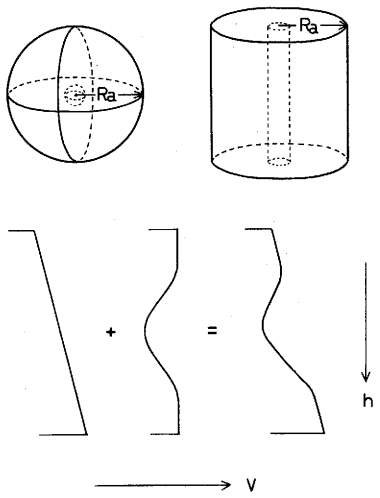

Fig. 5. Low-velocity body models: Spherical and cylindrical bodies. The velocity anomaly cores within the bodies are shown by dotted lines. The velocity anomaly is modeled as illustrated in the lower figure employing the function (1) in the text. **v** and **h** denote P velocity and depth.

for the low-velocity body: spherical and cylindrical bodies (Fig. 5). The P velocity within the body v is assumed to take the form:

$$\begin{aligned} v &= V_b + V_0 \cdot \varepsilon, && r \leq R_c \\ &= V_b + V_0 \cdot \varepsilon \cdot \cos^2\left(\frac{\pi}{2}\frac{r-R_c}{R_a-R_c}\right), && R_c \leq r \leq R_a \end{aligned} \tag{1}$$

where R_a and R_c are radii of the body and the core, respectively; V_0, V_b are the background standard velocities at the center of the body and at the specified point with radius r within the body, respectively; ε means the degree of anomaly. Such a continuously differentiable function as square of cosine function would be necessary for stabilizing the computation involved in ray tracing. This model construction is illustrated in Fig. 5. Model parameters are coordinates of the central position of the body, R_a, R_c, and ε. In the case of cylindrical model the position of the center is specified by only the horizontal one.

The computing algorithm for 3-D ray tracing is based on the program ANRAY86 (Gajewski and Pšenčik, 1986, 1987), where a system of ordinary differential equations is solved by the Runge-Kutta method. Amplitude change due to geometrical spreading is numerically estimated as follows. We take a small quadrilateral cross-sectional area perpendicular to the ray whose corners are crossing points of surrounding four rays on the hypothetical unit sphere centering the source. The elemental area is written as $\cos(\theta) \cdot 2\Delta\theta \cdot 2\Delta\varphi$, where $\Delta\varphi$, $\Delta\theta$ are small increments of azimuth and take-off angles, respectively. Next, we measure the area of the quadrilateral whose corners are made by the above four rays incident on the surface ground in the vicinity of the station.

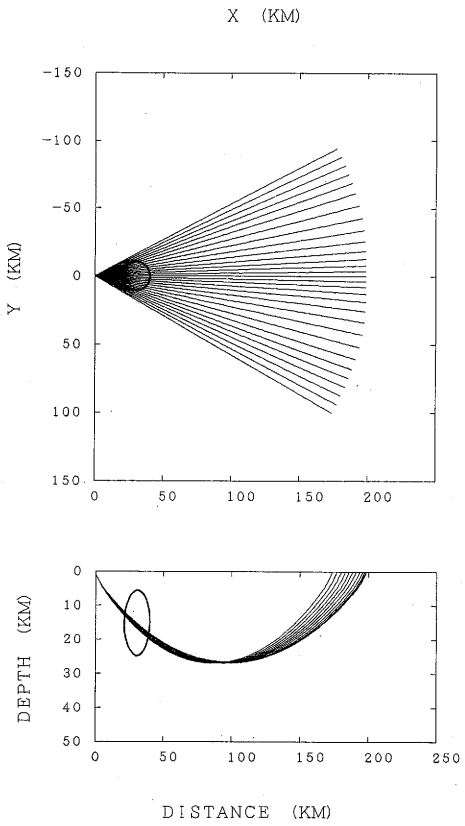

Fig. 6. Rays passing through the spherical low-velocity body. The center of the body is located at 30 km in epicentral distance and 15 km in depth. The solid circle shows the position and size of the body. Note that the depth scale is exaggerated. The parameters of the low-velocity body model are as follows: $\varepsilon=-0.03$, $R_a=10$ km, and $R_c=0$ km. Upper: Horizontal projection of rays with a constant take-off angle of 39.1° from the horizontal plane. Lower: Rays on the vertical plane crossing the center of the body.

The square root of the ratio of the area at the source to that at the station gives the relative amplitude of the vertical component of seismic wave. We adopted $\Delta\varphi=\Delta\theta=0.5°$ in the computation throughout this paper: tests have been made to confirm no noticeable change in computed amplitudes for various angle sizes between 0.1° and 0.5°.

Figure 6 shows an example of ray pattern for a spherical low-velocity model. The high density of rays implies the focusing of wave energy and the low density manifests defocusing. The ray emitted at a take-off angle of 39.1° from the horizon reaches to the ground surface at an epicentral distance of 200 km provided that we use the velocity model (b) given in Fig. 4. The center of the large scale magma body should be located at depths below about 10 km where we have no definite seismicity (e.g., Tohoku

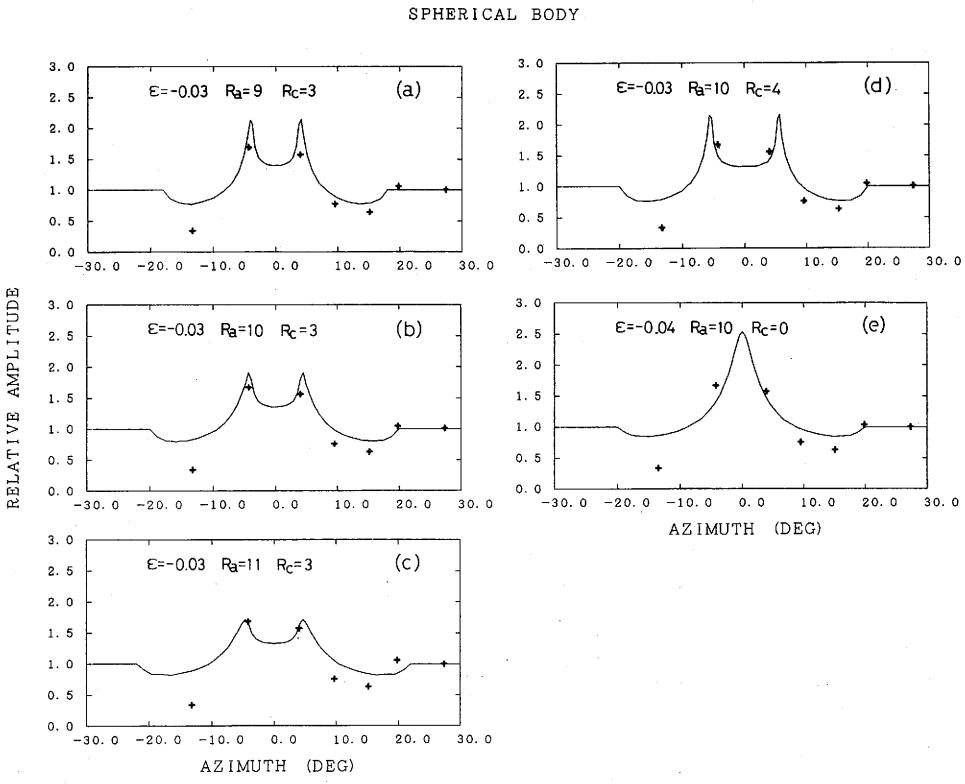

Fig. 7. Theoretical azimuthal amplitude distributions for the spherical body models. The azimuth is measured from the direction N45.8°W clockwise. The center of the body is located at 30 km in epicentral distance and 15 km in depth. The observational data are indicated by +. The rays are computed for a constant take-off angle of 39.1°. Values for model parameters are shown in each figure. Numerals for R_a and R_c are in km.

University, 1990). If we take the depth as 15 km and assume that the central ray propagates through there, then the center of the body is located 30 km in epicentral distance. The azimuth of this location is assumed to be N45.8°W, the mid direction between the two stations TKN and ASI. Figures 7 and 8 show the examples of the numerical results based on the above assumption.

Computed amplitude distributions have a peak at the center and troughs outside it. A splitted peak or double peaks appear for the non-zero core radius R_c. The total size R_a determines the range of the side troughs. Fitting is better for these troughs in the case of the cylindrical body model than the spherical one. As discussed later, the wave amplitudes behind the low-velocity body are reduced by about 10% by the attenuation. Therefore, we have to make a small correction by raising amplitudes around the peak. The observed data except for the left end station, TKC, are in good agreement with the theoretical ones for the cylindrical model with the parameters:

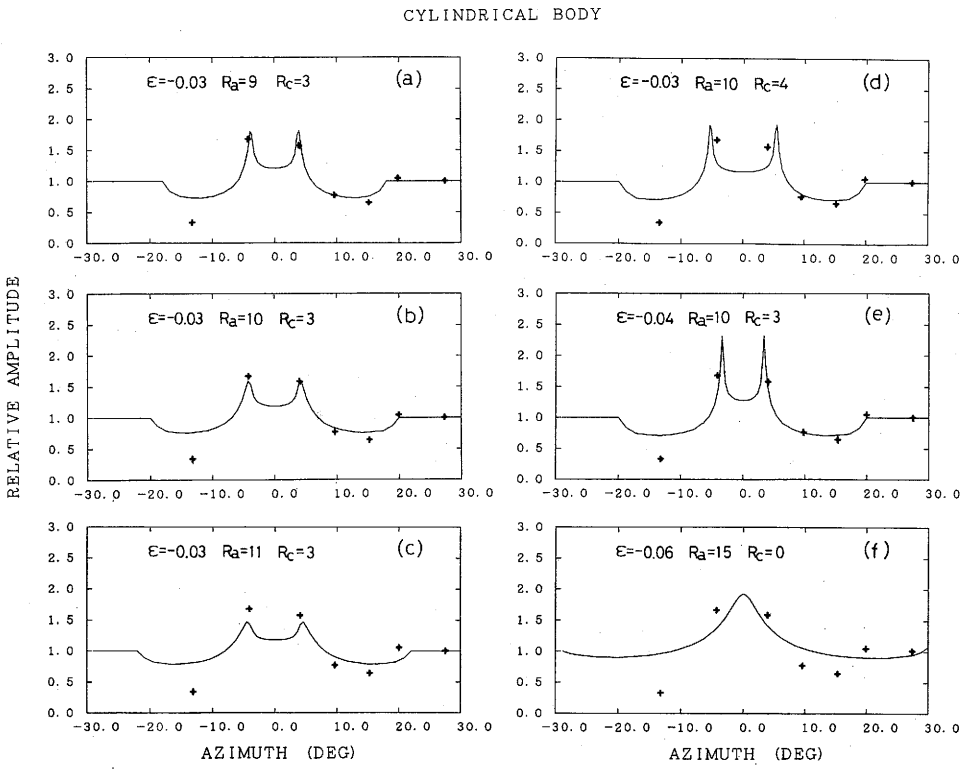

Fig. 8. Theoretical azimuthal amplitude distributions for the cylindrical body models as similar as Fig. 7.

$\varepsilon = -0.04 \sim -0.03$, $R_a = 10$ km and $R_c = 3$ km (Fig. 8(b), (e)).

In order to see whether or not other model solutions would be possible, we change the location of the low-velocity body to some extent. If we move the body 10 km further in epicentral distance, an optimum solution is obtained for the cylindrical model as shown in Fig. 9(a). In this case the ray penetrates the body at a depth of 18 km. The cylindrical model predicts the similar radiation pattern even if we take the observation distance as 230 km, corresponding to the far stations concerned (Fig. 9(b)). For the spherical model, we are generally required to change the depth of the body center along with the distance. However, a slight change of the distance yielded a solution without changing the depth (Fig. 9(c)).

It is easy to extend our velocity body model to an elliptical shape. A cylindrical model with an elliptical horizontal cross section elongating in the radial direction from the epicenter makes such a complex radiation pattern as triple peaks, whereas a transversely extended elliptical cylinder is difficult to produce predominant peaks. Even if we take this model, the rough size and degree of velocity anomaly are not greatly changed.

On the other hand, the travel time anomalies expected theoretically are much

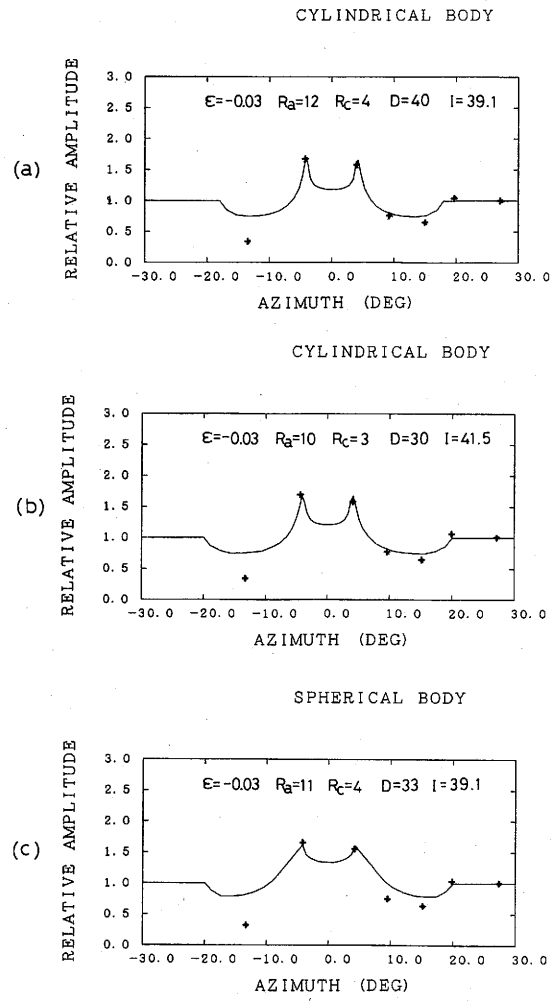

Fig. 9. Theoretical azimuthal amplitude distributions for the spherical and cylindrical body models. **D** and **I** are horizontal distance in km from the source and take-off angle in degree measured from the horizon. Notation of other parameters is the same as Figs. 7 and 8. The take-off angle 41.5° in (b) implies the epicentral distance of 230 km at the station. The depth of the spherical body in (c) is 15 km as in Fig. 7.

smaller than the observed ones (Fig. 10). The excess of the anomalies should be attributed to the heterogeneity of the medium in the wider area than the low-velocity body that we modeled. The low-velocity zone may be spread out in the Izu Peninsula as indicated in the travel time delay data.

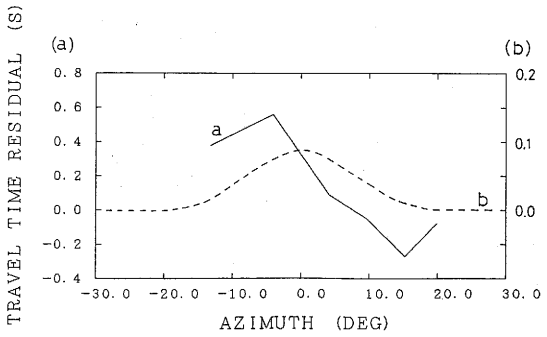

Fig. 10. Travel time residuals. The observational data (a) are shown by solid line and with the left-hand side vertical scale; the theoretical ones (b) by broken line and with the right-hand side scale.

4. Discussion

Before entering into the discussion about the implication of the model presented in the last section, let us examine our data from several aspects. First, why did we restrict the waveform data from the stations with a short range of epicentral distances? It is because the limited range of take-off angle assures the assumption of the equal strength of radiation against the azimuth, and the configuration of stations at about a 200 km distance was really available. Actually, one more station would be available if the ground noise level was small enough to identify the waveform signal. The station YKE of Nagoya University is located at the distance of 237.5 km in the direction of N43.8°W between TKN and ASI in the azimuth. However, the amplitude may be less than that of the two neighboring stations supporting the splitted peak.

Secondly, can we neglect the effect of the absorption of energy at the low-velocity body? Low velocity means low Q at the same time. When we assume the Q value as 50, then the amplitude would reduce by about 12% according to the formula $\exp(-\pi f t/Q)$, where f, the frequency of wave, is equal to 0.65 Hz and t, the propagating time, 3 s. For Q values greater than 300, which would be applied to the surrounding regions, the reduction is not more than 3%. Furthermore, the amplitude measurements are believed to have an error of as much as about 10%. We should take these uncertainties into accout in the applications of the amplitude data.

Thirdly, can we neglect the other velocity structures along the ray paths? A magma reservoir is estimated to exist centering at the place 3 km northwest of the summit crater of Mt. Mihara at a depth of 5 km (Ida *et al.*, 1988 a). The rays go through about 1 km above this center. However, the effect turns out to be very small causing less than several percent fluctuation of amplitude variation provided that the low-velocity body size is several kilometers in radius and the degree of the anomaly is 3–4%. Besides this, other magma bodies beneath such a volcano as Mt. Fuji may presumably affect the wave propagation. It is quite difficult to evaluate their effects because we have no reliable information concerning their locations.

The essential part of our interpretation of the data is the proposal of the presence

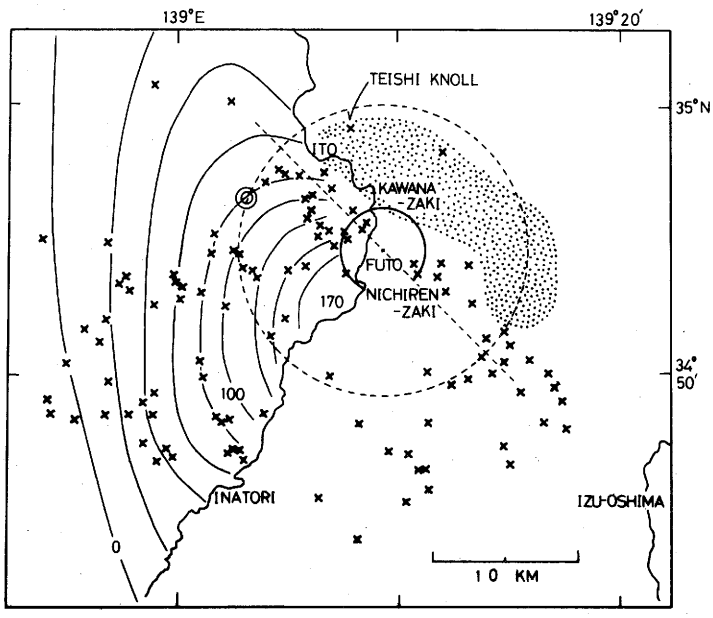

Fig. 11. Volcanologic and geodetic map around the eastern Izu Peninsula and Izu-Oshima Island. The dotted line describes the possible location of the low-velocity center. The most probable position of the core of the low-velocity area with 3% anomaly is indicated by a circle drawn with the solid line. The dotted circle represents the entire size of the low-velocity body. The shaded zone by dots shows the outline of the source area of the earthquake swarms (January 1987 to October 1988; after Earthquake Research Institute, 1989). Vents of the Higashi-Izu monogenetic volcano group (after Aramaki and Hamuro, 1977) are indicated by ×. The Teisi Knoll, the spot of the 1989 submarine volcanic eruption, is also plotted after Maritime Safety Agency (1990). The contour lines on the land, Izu Peninsula, indicate the uplift of the ground during the period from 1980 to 1988 in mm after Ishii (1989). The open double circle indicates the uplift center during the period from 1967 to 1978 after Geographical Survey Institute (GSI, 1978).

of the low-velocity center along the line in the direction of N45.8°W. It is not easy to constrain its very point. We have to rely on the other evidence. The recent uplifting crustal movement might indicate the activity of the presumable magma reservoir. The most simple model to explain this is the so-called Mogi's Model. Hagiwara (1977) calculated the parameters of the spherical cavity pressure source model: The depth should be 10 km and the radius 3 km for the 1967–1978 upheaval centering on Hiekawa, 6 km southwest of Ito, with the maximum vertical displacement of 16 mm. Following the above crustal movement, the recently accumulated ground deformation revealed the uplift peak around Futo, between Kawana-zaki and Nichiren-zaki, the eastern coast of Izu Peninsula, with a considerably high rate of 170 mm during 8 years (Ishii, 1989;

Fig. 11). It is quite probable that the magma reservoir or the low-velocity center is located close to that region as shown in Fig. 11.

The source area of the frequent earthquake swarm takes place around northeastern part of the transition zone of the low velocity body. Reliable depth distributions of the swarm earthquakes of 1989 and 1930 were recently determined by using a dense seismic network and a revised crustal structure model (Ueki *et al.*, 1990). The lower limit of the seismicity is about 10 km.

The proposed low-velocity center and the earthquake swarm source are close to the northeastern border of the region of Higashi-Izu monogenetic volcano group proposed by Aramaki and Hamuro (1977) (Fig. 11). This region is characterized by the scattered small separated Quaternary volcanoes. The recent magmatic and seismic activities in the north may imply that the active magma reservoir has been moving northward in recent geologic age.

The inactive old magma reservoir in the southern region may have remained as complicated low-velocity bodies even if the anomalies would be relatively weak. The preserved hot region is evidenced by the reflected arrivals of seismic waves that may indicate the presence of the reflectors, or the top of the magma reservoir (Mizoue *et al.*, 1989). The disclosed reflectors are widely distributed over the volcano group, with depths around 15 km. The above nature might reflect the large travel time anomalies and the disagreement between the theory and the observation at the southernmost station.

5. Conclusion

The anomalous amplitude distribution of seismic waves that originated from the eruption of Volcano Mihara in Izu-Oshima Island were observed at stations of about a 200 km epicentral distance. The focusing and defocusing effect of seismic rays passing through the magma reservoir explains well the above observation. The cylindrical body model is preferable to the spherical one for the magma reservior. The depth of its center would be 10–20 km. Its location is close to the northeastern border of the region of Higashi-Izu monogenetic volcano group. The radius of the low-velocity body around the reservoir is 10 km, the radius of the core of 3–4% anomaly being 3 km. This derivation was made by assuming an azimuthally isotropic radiation pattern at the source and weak heterogeneities of the medium other than the magmatic region.

The confirmation of the result in this paper using a large quantity of waveform data from nearer and more distant stations remains for future study. To do this we shall need more detailed knowledge of the source and the medium. It will involve a problem of general inversion.

The seismograms at the stations TKN and TKC are provided by Drs. Fumihito Yamazaki and Iwao Fujii at Nagoya University; the near-field seismograms at the stations in the Izu-Oshima Island by Prof. Hidefumi Watanabe and Dr. Koshun Yamaoka at the University of Tokyo; some arrival time data of seismic waves by Mr. Hiroo Wada at Kyoto University. The computer program by Dr. Dirk Gajewski was used making slight revision and reconstruction. Prof. Ichiro Kawasaki at Toyama University introduced this program to me. The above persons should be

greatly acknowledged. Hearty thanks are extended to anonymous reviewers for improvement of the manuscript.

REFERENCES

Aramaki, S. and K. Hamuro, Geology of the Higashi-Izu monogenetic volcano group, *Bull. Earthq. Res. Inst., Univ. Tokyo*, **52**, 235–336, 1977 (in Japanese).

Ashiya, K., S. Asano, T. Yoshii, M. Ishida, and T. Nishiki, Simultaneous determination of the three-dimensional crustal structure and hypocenters beneath the Kanto-Tokai District, Japan, *Tectonophysics*, **140**, 13–27, 1987.

Earthquake Research Institute, Seismic activities in the Izu Peninsula and its vicinity, *Rep. Coord. Comm. Earthq. Predict.*, **41**, 243–256, 1989 (in Japanese).

Fukuyama, E. and M. Takeo, Analysis of the near-field seismogram observed during the eruption of Izu-Oshima Volcano on November 16, 1987, *Bull. Volcanol. Soc. Jpn.*, **35**, 283–297, 1990 (in Japanese).

Gajewski, D. and I. Pšenčik, Numerical modeling of seismic fields in 3-D laterally varying layered anisotropic structures (Program ANRAY86), Internal Report, Institute of Earth and Planetary Physics, University of Alberta, 1986.

Gajewski, D. and I. Pšenčik, Computation of high-frequency seismic wavefield in 3-D laterally inhomogeneous anisotropic media, *Geophys. J. R. Astron. Soc.*, **91**, 383–411, 1987.

Geographical Survey Institute, Crustal deformation in Izu-Peninsula, *Rep. Coord. Comm. Earthq. Predict.*, **20**, 92–99, 1978 (in Japanese).

Hagiwara, Y., The Mogi model as a possible cause of crustal uplift in the eastern part of Izu Peninsula and the related gravity change, *Bull. Earthq. Res. Inst., Univ. Tokyo*, **52**, 301–309, 1977.

Ida, Y., K. Yamaoka, and H. Watanabe, Underground magmatic activities associated with the 1986 eruption of Izu-Oshima volcano, *Bull. Volcanol. Soc. Jpn.*, **33**, S307–S318, 1988 a (in Japanese).

Ida, Y., K. Yamaoka, and H. Watanabe, Model of volcanic activity associated with magma drain-back—Implication for eruptions of Izu-Oshima Volcano after December, 1986—, *Bull. Earthq. Res. Inst., Univ. Tokyo*, **63**, 183–200, 1988 b (in Japanese).

Ishii, H., Recent abnormal uplift on the Izu peninsula (1980–1988), *Bull. Earthq. Res. Inst., Univ. Tokyo*, **64**, 313–324, 1989 (in Japanese).

Jackson, P. S., The focusing of earthquakes, *Bull. Seismol. Soc. Am.*, **61**, 685–695, 1971.

Japan Meteorological Agency, Seismic activity in and around the Izu Peninsula (May–October, 1989), *Rep. Coord. Comm. Earthq. Predict.*, **43**, 140–156, 1990 (in Japanese).

Kuno, H., Geology and petrology of Omuro-yama volcano group, north Izu, *J. Fac. Sci., Univ. Tokyo, Sec. 2*, **9**, 241–265, 1954.

Maritime Safety Agency, Submarine topographic change related to submarine volcano eruption at Teisi Knoll off Ito in the eastern coast of Izu Peninsula, *Rep. Coord. Comm. Earthq. Predict.*, **43**, 323–334, 1990 (in Japanese).

Mizoue, M., I. Nakamura, I. Ogino, and T. Iidaka, Detection of S*x*P and S*x*S waves reflected from the deep crust in the eastern Izu Peninsula, Programme and Abstracts, the Seismological Society of Japan, 1989, No.2, 210, 1989 (in Japanese).

Nasu, N., Recent seismic activities in the Idu Peninsula (Part 2), *Bull. Earthq. Res. Inst., Univ. Tokyo*, **13**, 400–416, 1935.

Takeo, M., H. Yamasato, I. Furuya, and M. Seino, Analysis of long-period waves excited by the November 1987 eruption of Izu-Oshima Volcano, *J. Geophys. Res.*, **95**, 19377–19393, 1990.

Tohoku University, Earthquake Swarm off the east coast of the Izu Peninsula caused by volcanic eruption of the Teisi seamount, *Rep. Coord. Comm. Earthq. Predict.*, **43**, 182–190, 1990 (in Japanese).

Ueki, S., H. Hamaguchi, Y. Morita, and T. Nishizawa, Comparison between the 1930 and 1989 Ito Earthquake Swarm, Programme and Abstracts, the Seismological Society of Japan, 1990, No.2, 122, 1990 (in Japanese).

Watanabe, H., S. Okubo, K. Yamaoka, S. Sakashita, and T. Maekawa, Gravity changes after the 1986 eruption of Izu-Oshima Volcano, *Bull. Volcanol. Soc. Jpn.*, **33**, 224, 1988 (in Japanese).

Yamaoka, K., Y. Ida, K. Yamashina, and H. Watanabe, Seismicity and relation to the eruption of Izu-Oshima Volcano on November 1987, *Bull. Volcanol. Soc. Jpn.*, **34**, 263–274, 1989 (in Japanese).